Ground Truthing the Prediction of Water use by a Vineyard and Almond Orchard from Estimates of Canopy Cover Derived from Satellite measures of NDVI

Claire Williams

Flinders University South Australia

Supervised by Dr C Ewenz[1,2], Mr R Stevens[2] and Dr H Guan[1]

[1] Flinders University, School of the Environment (Earth Sciences), GPO Box 2100, Adelaide SA 5001

[2] SARDI/PIRSA Sustainable Systems, Wine Innovation Building, Cnr Hartley Grove and Paratoo Rd, Waite Precinct, Urrbrae SA 5064 (GPO Box 397, Adelaide SA 5001)

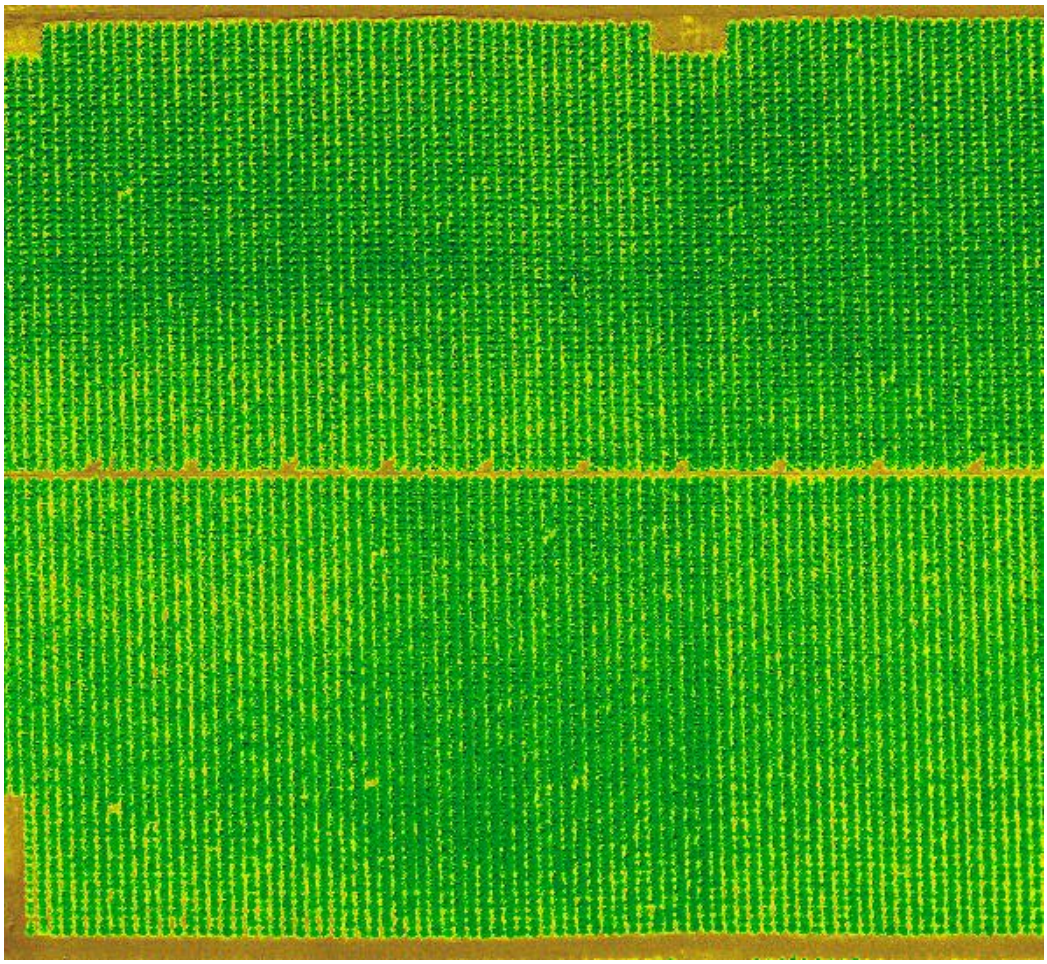

NDVI image of the almond orchard, Loxton, South Australia. The block shown here is approximately 600 m in east-west and 500 m in north-south distance. Image ARA (Airborne Research Australia), 27th of February 2007.

Contents

Table of Figures 2
1. Introduction 5
1.1. Background 5
1.2. Measures of Crop Water Use 7
2. Method 8
2.1. Vegetation Index 8
2.2. Acquisition of NDVI 10
2.3. Post Acquisition Processing 12
3. Results 13
3.1. The Vineyard 13
3.2. The Almond Orchard 16
4. Conclusion 19
5. References 20
Appendix 1 - Evapotranspiation 21
Appendix 2 - Footprints 24
Appendix 3 - Soil Water Content 26
Appendix 4 - Pre-dawn Leaf Water Potential 27
Appendix 5 - Satellite Overpasses 28
Appendix 6 - Collecting MODIS data 29

Table of Figures

Figure 1: The estimated absorption spectra used by plants (Maryland, 2008). 9
Figure 2: The vegetation index – healthy and stressed vegetation reflectance (ODIS, 2007). 9
Figure 3: The vineyard at Loxton (ORNL, 2010). 11
Figure 4: The almond orchard at Loxton (ORNL, 2010). 11
Figure 5: The seasonal course of NDVI from the Terra (morning) and Aqua (afternoon) data for the well watered, own rooted Chardonnay vineyard every 16 days. The fruit was harvested for sparkling wine in early February. 13
Figure 6: The seasonal course of NDVI from the Terra (mid-morning) satellite overpass, the averages for the same sampling dates of the ratio ET:ETo for the hour periods which encompass the time of the satellite overpass, and the 24 hour period including the time of the satellite overpass. 14
Figure 7: The seasonal course of NDVI from the Aqua (early-afternoon) satellite overpass, the averages for the same sampling dates of the ratio ET:ETo for the hour periods which encompass the time of the satellite overpass, and the 24 hour period including the time of the satellite overpass. . 14

Figure 8: The relationship between the 16 day averages of daily ET/ETo and NDVI's derived from Terra (morning) and Aqua (afternoon) satellite overpasses. 15
Figure 9: The relationship between 16 day average of daily ET/ETo and FAO Kc's for the wine grapes vineyard. 15
Figure 10: The seasonal course of NDVI from the Terra (morning) and Aqua (afternoon) data for 16 day periods for a well watered almond orchard. The almonds were harvested in March. 16
Figure 11: The seasonal course of NDVI from a mid-morning satellite overpass, the averages for the same sampling dates of the ratio ET:ETo for the hour period which encompasses the time of the satellite overpass and for the 24 hour period including the time of the satellite overpass..... 17
Figure 12: The seasonal course of NDVI from a early-afternoon satellite overpass, the averages for the same sampling dates of the ratio ET:ETo for the hour period which encompasses the time of the satellite overpass and for the 24 hour period including the time of the satellite overpass..... 17
Figure 13: The relationship between 16 day averages of daily ET/ETo and NDVI's derived from Terra (morning) and Aqua (afternoon) satellite overpasses. 18
Figure 14: The relationships between 16 day averages of daily ET/ETo and FAO Kc's for the almond orchard. 18
Figure 15: The relationship between ET (blue dots), ETo (red dots) and Kc (green dots) for the 16 day average hourly (morning) period for the well watered vineyard, Styles, Stevens & Grigson (unpublished data). 21
Figure 16: As in Figure 15 but for the hourly (morning) period for the well watered almond orchard, Ewenz, Stevens & Grigson (unpublished data). 21
Figure 17: As in Figure 15 but for the hourly (afternoon) period for the well watered vineyard, Styles, Stevens & Grigson (unpublished data). 22
Figure 18: As in Figure 15 but for the hourly (afternoon) period for the well watered almond orchard, Ewenz, Stevens & Grigson (unpublished data). 22
Figure 19: As in Figure 15 but for the 24 hour period for the well watered vineyard, Styles, Stevens & Grigson (unpublished data). 23
Figure 20: As in Figure 15 but for the 24 hour period for the well watered almond orchard, Ewenz, Stevens & Grigson (unpublished data). 23
Figure 21: The ET-weighted composite measurement footprints showing approximately 85% of the area of influence for each month of measurements from February 2007 to January 2008 for the vineyard. Block length is approximately 400 m in the *x* direction and 280 m in the *y* direction. The red parallelogram overlaying the top left footprint exhibits the satellite tile, Styles, Stevens & Grigson (unpublished data). 24
Figure 22: The ET-weighted composite measurement footprints showing approximately 95% of the area of influence for each month of measurements from September 2008 to May 2009 for the almond orchard. Indicated is the orchard section (northern rectangle, 200m by 250m) for the EC tower. The red parallelogram overlaying the top left footprint exhibits the satellite tile, Ewenz, Stevens & Grigson (unpublished data). 25
Figure 23: The root weighted soil water content 0 to 120cm depth in the vineyard, Styles, Stevens & Grigson (unpublished data). 26
Figure 24: The soil water content average over 0 to 100cm depth in the almond orchard, Ewenz, Stevens & Grigson (unpublished data). 26
Figure 25: The variation in grapevine dawn leaf water potential with soil water content, Styles, Stevens & Grigson (unpublished data). 27

Figure 26: The variation in almond pre-dawn leaf water potential with soil water content, Ewenz, Stevens & Grigson (unpublished data). 27
Figure 27: Terra's predicted pathway; passes on 1/5/2008. The time is in universal time coordinated (UTC) (SSEC, 2010). 28
Figure 28: Aqua's predicted pathway; passes 1/4/2008. The time is in universal time coordinated (UTC) (SSEC, 2010). 28
Figure 29: Map of the earth (ORNL, 2009)..... 29

I would like to thank Dr Caecilia Ewenz, Mr Rob Stevens and Dr Huade Guan for their help and support on this project.

1. Introduction

1.1. Background

The Murray Darling Basin is Australia's largest agricultural area and a major user of water for irrigation. The Basin's capacity to supply water is fast reducing due to increased extraction for industrial uses, domestic supply and, most significantly, agricultural irrigation. The Basin contains approximately 72% of Australia's irrigated crops; therefore irrigation needs to become more efficient in order to match supply with demand (MDBMC, 2007).

Recent droughts have increased investment in improving irrigation efficiency. A common measure of this efficiency is the ratio of seasonal crop water use to seasonal irrigation application. In order to assess whether increased investment is improving efficiency we need to develop accurate estimates of the rate of water use at the individual crop and district level.

The rate of water used by a crop, ET = evapotranspiration, depends on weather, growth stage and soil water availability. Crop yield is a function of water use. Crop water use can be estimated under well watered conditions as a function of reference crop evapotranspiration (ETo) and a set of crop coefficients. The coefficients (Kc) are crop specific. Crop evapotranspiration (ETc) is estimated as the product of the rate of reference crop evapotranspiration and the appropriate crop coefficient (ETc = ETo X Kc) (Allen et al., 1998). However the crop coefficient does not account for variations in canopy cover between different areas.

Reference crop evapotranspiration (ETo) is the evaporation from a grass reference crop without a shortage of water that shows certain characteristics (Allen et al., 1998). Climatic parameters are the only factors affecting ETo and so ETo can be calculated from weather data. The variations in the values of ETo with location and season reflect the temporal and spatial variation in the evaporative influence of the atmosphere. These values are not dependent on soil characteristics (Allen et al., 1998).

Evapotranspiration (ET) is the sum of evaporation and transpiration. It is the transport of water into the atmosphere from the earth's surface. It is one of the main consumers of solar energy at the earth's surface and is one of the most significant components of the

hydrological cycle. The energy used for ET is often referred to as the latent heat flux (Burba et al., 2006).

Evaporation is the process whereby water is directly returned back into the atmosphere through evaporative loss from soil surfaces, standing water and other water surfaces. Transpiration is the process in which water is used by vegetation and consequently lost back to the atmosphere as water vapour. The water enters through the root zone of the plant and is then used for different biophysiological processes such as photosynthesis. Water then passes back to the atmosphere through the leaf stomata in the form of vapour. If the leaf becomes stressed to the wilting point, transpiration will stop (Burba et al., 2006).

Evapotranspiration is a function of soil water content (SWC), crop stage and canopy cover (CC). Matching supply with demand is a function of the rate at which water is being used by the plant and how water is being stored in the root zone. Supply will depend on SWC the sufficiency of which can be inferred from measurements of pre-dawn leaf water potentials, while water demand is dependent on crop growth stage and ET.

The eddy covariance technique (EC) is an atmospheric flux measurement technique used to measure and calculate vertical turbulent fluxes including wind speed within atmospheric boundary layers. An eddy covariance system generally measures carbon dioxide, air temperature, moisture and 3-D wind speed above a crop canopy. The net moisture flux is a result of soil evaporation plus plant transpiration minus precipitation and condensation (Glen et al., 2008). The EC measurement represents the flux from a specific area of crop. The size and location of this area relative to the tower site depends on wind speed, wind direction, atmospheric stability and tower height above the canopy. The area is called flux footprint and is the upwind area which is the source of the atmospheric flux measured by the instruments (Glen et al., 2008).

The main source of variation in the tabulated values of Kc is the growth stage. At a given growth stage, the rate of water use by an individual vine, for example, is proportional to its canopy cover. However the tabulated values of Kc do not account for canopy cover variations between vineyards. The canopy cover of a vineyard can be estimated from remotely acquired measures of vegetative indices.

Vegetation indices are derived from measures of the way that plant canopies modify light radiation. The normalised difference vegetation index (NDVI) is a widely known example of such an index. The NDVI is a numerical indicator used to detect live green plant canopies in multi-spectral remote sensing data. It is an index used to identify the condition of vegetation in different areas. The NDVI is calculated from the visible and near-infrared light reflected by vegetation (Weier and Herring, 2010).

The NDVI can be used as a measure of canopy cover (CC). Trout and Johnson (2007) and Trout et al. (2008) have shown that there is a strong connection between NDVI and CC as NDVI was found to increase linearly with canopy cover up to approximately 0.8. Therefore NDVI can be used as a surrogate for measures of CC.

Ayars et al. (2003), Williams and Ayars (2005) and Goodwin et al. (2006) have shown that the crop water use of individual peach trees (which show similar characteristics to almond trees) and vines is linearly related to projected canopy cover.

Evapotranspiration data were collected using eddy covariance towers in a vineyard and an almond orchard between February 2007 and June 2009 in South Australia's Riverland. The project aimed to use these comprehensive data sets to explore whether the water use of an entire vineyard and an entire almond orchard can be estimated from reference crop evapotranspiration and crop coefficients adjusted with satellite measures of NDVI to account for variations in canopy cover.

1.2. Measures of Crop Water Use

The crop water status (well watered or otherwise), was determined from the relationship between a plant water status indicator (pre-dawn/dawn leaf water potential) and SWC (Appendix 4). These measures of plant water status indicators showed that at SWC greater than 15% (w/v) in the almond orchard and 14% (w/v) in the vineyard, the crops were well watered.

Appendix 3 shows the time course of SWC in the vineyard and almond orchard. The SWC in the vineyard was below 14% (w/v) during March and the start of April in 2007. The vines were dormant from May until the end of August 2007. Bud burst, that is, when leaves started to emerge took place on the 31/08/2007. Harvest commenced on the 4/02/2008.

Between bud burst and harvest the SWC was greater than 14% (w/v). In the almond orchard leaves started emerging near the end of flowering 31/08/2008, harvest took place on the 7/03/2009 and the irrigation season ended on the 22/04/2009. Leaf fall took place in late May. From leaf emergence till early April 2009 the SWC remained above 15% (w/v).

This study will focus on the data from periods when the crops were well watered which was between leaf emergence and harvest. For the vineyard this was between the 31/08/2007 and the 4/02/2008 and for the almond orchard this was between 1/09/2008 and the 7/03/2009.

The monthly footprints, or source area, of the information obtained from the eddy covariance measurements is shown in Appendix 2.

2. Method

2.1. Vegetation Index

Many different wavelengths make up the spectrum of light. When sunlight hits an object, some wavelengths of the spectrum are absorbed and others are reflected. The pigment in plant leaves, chlorophyll, strongly absorbs visible light (from 0.4 to 0.7µm, but with little absorption in the green colour) to use in processes such as photosynthesis, see Figure 1. The cell structure of leaves strongly reflects near-infrared light (from 0.7 to 1.1µm) (Weier and Herring, 2010).

A vegetation index can be calculated by measuring the wavelengths and intensity of visible (VIS) and near-infrared (NIR) sunlight reflected by vegetation back to space (Weier and Herring, 2010).

The normalized difference vegetation index (NDVI) is a relation between the NIR and RED spectral bands, see Figure 1 and Figure 2. The chlorophyll (green pigment) absorbs incoming radiation in the visible band, while the leaf structure and water content is responsible for a high reflectance in the near infrared region of the electromagnetic spectrum (Weier and Herring, 2010).

The photosynthetically active radiation (PAR) designates the spectral range (wave band) of solar radiation from 0.4 to 0.7µm that photosynthetic organisms use in the process of photosynthesis. This spectral region corresponds approximately with the spectrum of light visible to the human eye (Weier and Herring, 2010). Leaf cells reflect and emit radiation in the near infrared spectral region. Live, healthy green plants will appear dark in the PAR and bright in the NIR while clouds and snow will appear dark in the NIR and bright in the PAR (Towson, 2010).

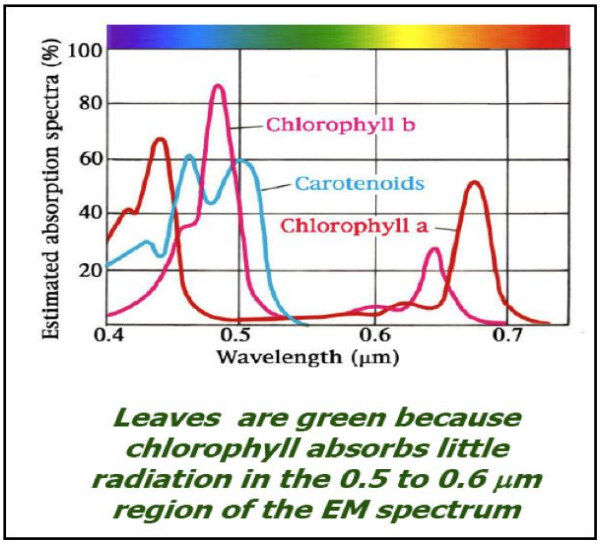

Figure 1: The estimated absorption spectra used by plants (Maryland, 2008).

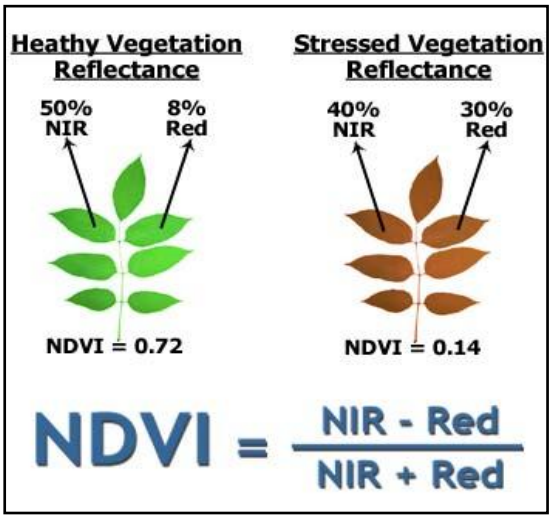

Figure 2: The vegetation index – healthy and stressed vegetation reflectance (ODIS, 2007).

The NDVI index ranges from -1 to 1. Green vegetation will have positive values while snow and clouds will have negative values (Weier and Herring, 2010). Dense vegetation reflects

more radiation in the near-infrared wavelengths than in the visible wavelengths (Weier and Herring, 2010).

2.2. Acquisition of NDVI

MODIS (Moderate Resolution Imaging Spectroradiometer) is an instrument onboard the Terra and Aqua satellites. These satellites view the whole earth's surface every 1-2 days. Terra orbits in descending node at 10:30am and Aqua orbits in ascending node at 1:30pm at local solar time at the equator (Weier and Herring, 2010). MODIS collects data in 36 spectral bands ranging in wavelength from 0.4µm to 14.4µm and at varying spatial resolutions: 2 bands at 250m, 5 bands at 500m and 29 bands at 1km. The overpass paths of the Terra and Aqua Satellites are shown in Appendix 5.

MODIS products are distributed using the sinusoidal projection in 10^{o} tiles. Daily scenes have geographic coordinates information embedded in the file (Yale, 2007). MODIS data was collected through the Oak Ridge National Laboratory Distributed Active Archive Centre (ORNL DAAC) website (ORNL, 2009). Detailed instructions on collecting MODIS data are given in Appendix 6.

The products were chosen from this site as the data is free and open to the public. The radiation data is already processed for atmospheric interferences. The vegetation indices, such as NDVI and EVI (Enhanced Vegetation Index), are calculated and ready to use in scientific research.

Raw data obtained through the ORNL DAAC website (ORNL, 2010) was sorted into an Excel spreadsheet to give the blue band, red band, near-infrared band, the NDVI and the EVI for the years between 2002 and 2009. This was done for both the morning (Terra) and afternoon (Aqua) data.

The measures of NDVI were used to explore variation in the measures of the crop coefficient Kc obtained from the ET and ETo using the eddy covariance technique.

Figure 3 shows the tile used to obtain the NDVI for the vineyard. The location is centred on latitude [$-34^{o}37'39''$] longitude [$140^{o}38'4''$]. The tile is approximately 250m wide and 250m high. The tile is located primarily within the vineyard planted to Chardonnay with the

eastern corner overlapping into a vineyard containing Shiraz. The footprint of eddy co-variance measures mostly lay within the area delineated by the tile (Appendix 2).

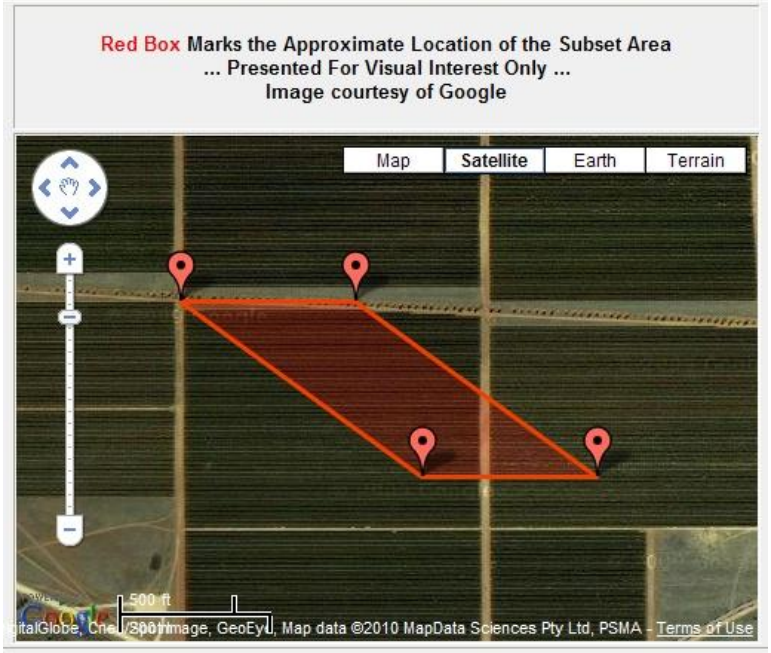

Figure 3: The vineyard at Loxton (ORNL, 2010).

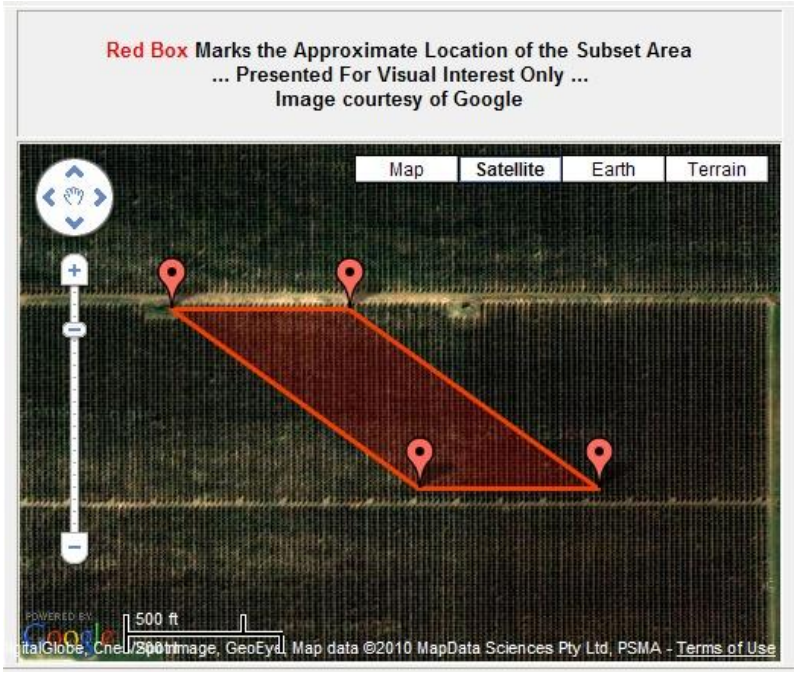

Figure 4: The almond orchard at Loxton (ORNL, 2010).

Figure 4 shows the tile used to obtain the NDVI for the almond orchard. The location is centred on latitude [-34°31'47"] longitude [140°39'19"]. The tile is approximately 250m wide and 250m high. The site of interest is surrounded by other almond orchard blocks

which are identical with regard to cultivar mix and age, and are subject to the same cultural management, so the vegetation indices should be representative of almond canopy within the footprint of the eddy covariance instrumentation, even though the tile does overlap with another orchard block. The footprint of eddy co-variance measures mostly lay within the area delineated by the tile (Appendix 2).

2.3. Post Acquisition Processing

The NDVI data from MODIS is given every 16 days with a timestamp of the first acquisition day. The on ground Kc 16 day average is thus calculated the same way using the 16 days after each date.

Evapotranspiration measurements are taken every half hour. The measurements for 10:30am, approximately corresponding with the Terra data, and at 1:30pm, Aqua overepass data, were chosen, and an average for these times for each day was taken. That is, an average between 10am and 11am to obtain a 10:30 reading and an average between 1pm and 2pm to get a 1:30pm reading for both ET and ETo. A 24 hour daily average was also calculated for ET and ETo to be used with a combination of Terra and Aqua data. For each of the morning, afternoon and daily values a 16 day running average was determined for both ET and ETo. This was to correspond with the MODIS data which is calculated using a 16 day average. Once a 16 day average had been calculated Kc could be determined as ET/ETo for the well watered crop.

The last data point for the vineyard results is not a full 16 day average, as only the data for the well watered crop was used and the vineyard evapotranspiration data did not cover the entire period of the well watered crop.

Although the MODIS data is captured in 16 day averages for both Aqua and Terra, the two averages are not calculated in the same 16 day cycles, but rather on alternative cycles 8 days apart. This means the Aqua and Terra dates do not match up for each value, which can be seen in Figure 5 and Figure 10**Error! Reference source not found.**. Therefore when looking at the relationship between the NDVI, ET/ETo and the 24 hour period, the dates for the 24 hour period were adjusted to match either NDVI Terra or Aqua and ET/ETo morning or afternoon.

The NDVI between the 28/08/2008 and the 10/06/2009 was chosen to correspond with the data from the almond orchard. The above method was also used to obtain the vegetation indices between the 13/02/2007 and the 20/01/2008 to correspond to the vineyard. The vegetation indices were then compared to the crop coefficient Kc for both the almond orchard and the vineyard using only the periods when the crops were well watered.

3. Results

3.1. The Vineyard

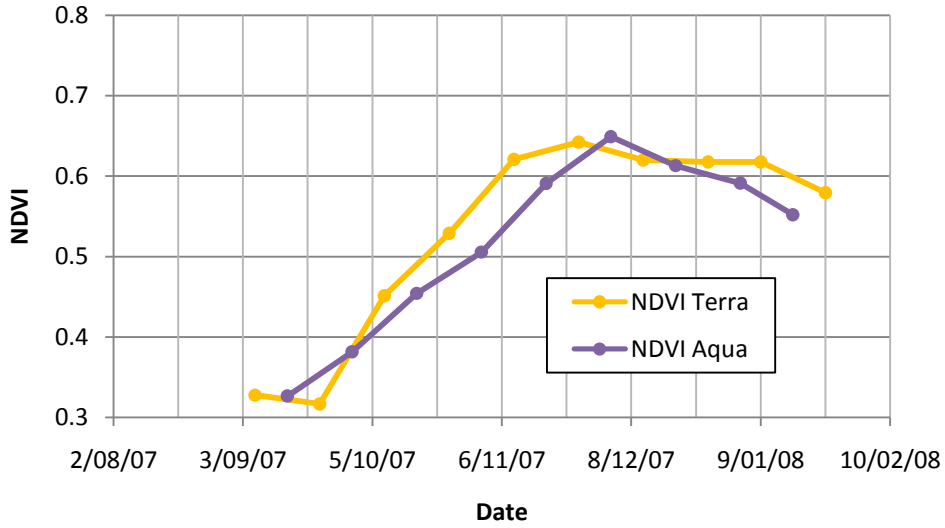

Figure 5: The seasonal course of NDVI from the Terra (morning) and Aqua (afternoon) data for the well watered, own rooted Chardonnay vineyard every 16 days. The fruit was harvested for sparkling wine in early February.

The seasonal course of values of NDVI determined from mid-morning overpasses of the Terra satellite is similar to that from early afternoon overpasses of Aqua satellite, Figure 5. Both measures of NDVI reach their peak value in early December.

The seasonal course of the NDVI derived from the mid-morning satellite overpass aligned with the seasonal course of the ratio of ET:ETo determined for the hour period (which encompassed the time of the satellite overpass) and for the 24 hour period see Figure 6. Prior to December, alignment between measures of NDVI and ratios of ET:ETo was not as strong.

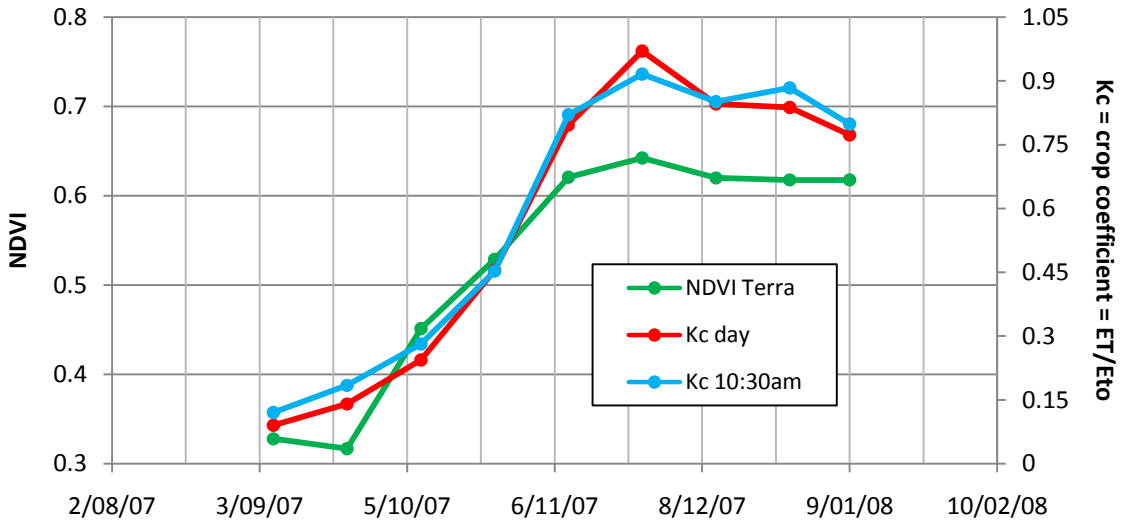

Figure 6: The seasonal course of NDVI from the Terra (mid-morning) satellite overpass, the averages for the same sampling dates of the ratio ET:ETo for the hour periods which encompass the time of the satellite overpass, and the 24 hour period including the time of the satellite overpass.

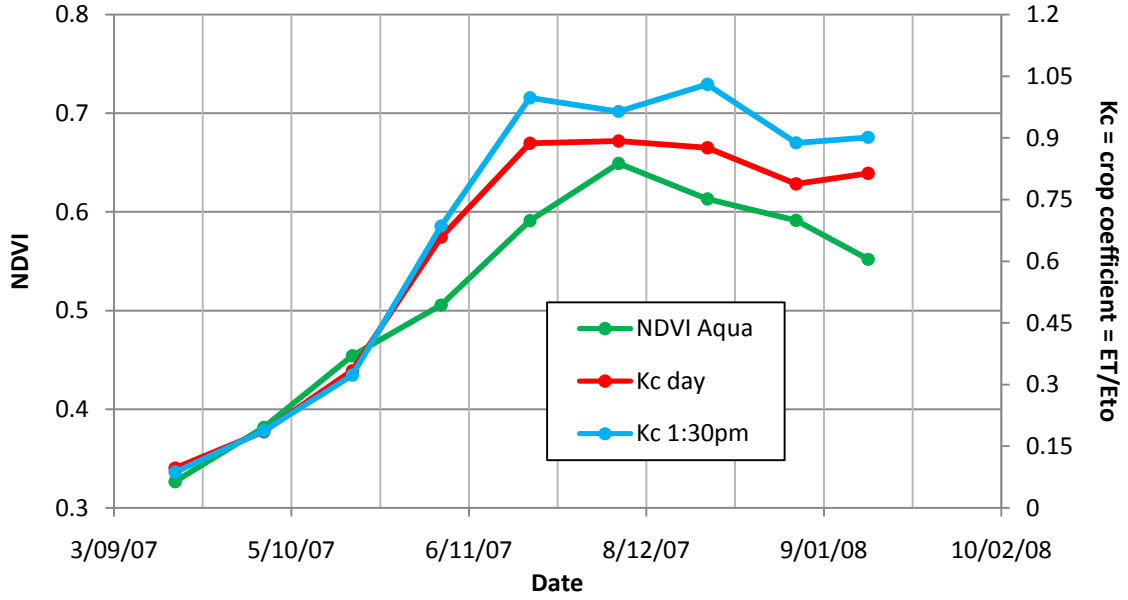

Figure 7: The seasonal course of NDVI from the Aqua (early-afternoon) satellite overpass, the averages for the same sampling dates of the ratio ET:ETo for the hour periods which encompass the time of the satellite overpass, and the 24 hour period including the time of the satellite overpass.

Likewise the seasonal course of NDVI derived from the early-afternoon satellite overpass aligned with the seasonal courses of the ratio of ET:ETo determined for the hour period (which encompasses the time of the satellite overpass) Figure 7.

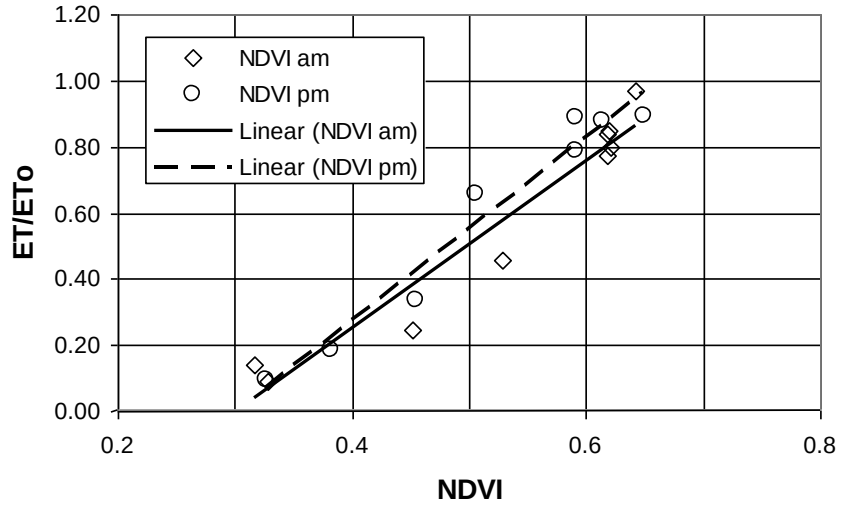

Figure 8: The relationship between the 16 day averages of daily ET/ETo and NDVI's derived from Terra (morning) and Aqua (afternoon) satellite overpasses.

The slopes and intercepts of separate regressions of ET/ETo on NDVI from morning and afternoon satellite overpasses were not significantly different, see Figure 8. The data was bulked and the overall regression equation between 16 day average daily ET/ETo for NDVI determined from either the morning or afternoon satellite overpasses was

ET/ETo = 2.62*NDVI-0.79 (r^2=0.93, n = 17, *P*<0.001).

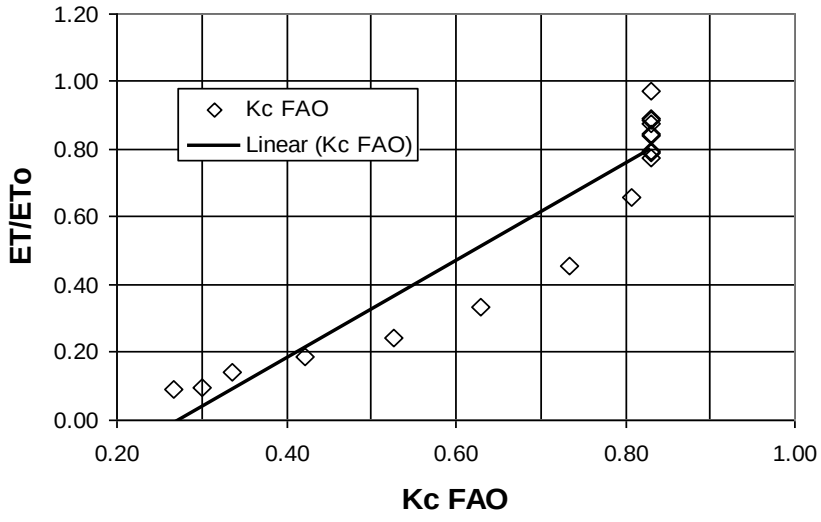

Figure 9: The relationship between 16 day average of daily ET/ETo and FAO Kc's for the wine grapes vineyard.

Figure 9 shows the relationship between the FAO Kc values (which have been adjusted to account for deviation of minimum RH and wind speed from standard conditions) and ET/ETo

for the same period. The overall regression equation between 16 day average daily ET/ETo for the Food and Agriculture Organization (FAO) wine grape vineyard Kcs was

ET/ETo = 1.44*Kc-0.39 (r^2=0.89, n = 17, *P*<0.001),

NDVI was a better predictor of the ratio of ET/ETo than the FAO Kcs for the wine grape vineyard.

3.2. The Almond Orchard

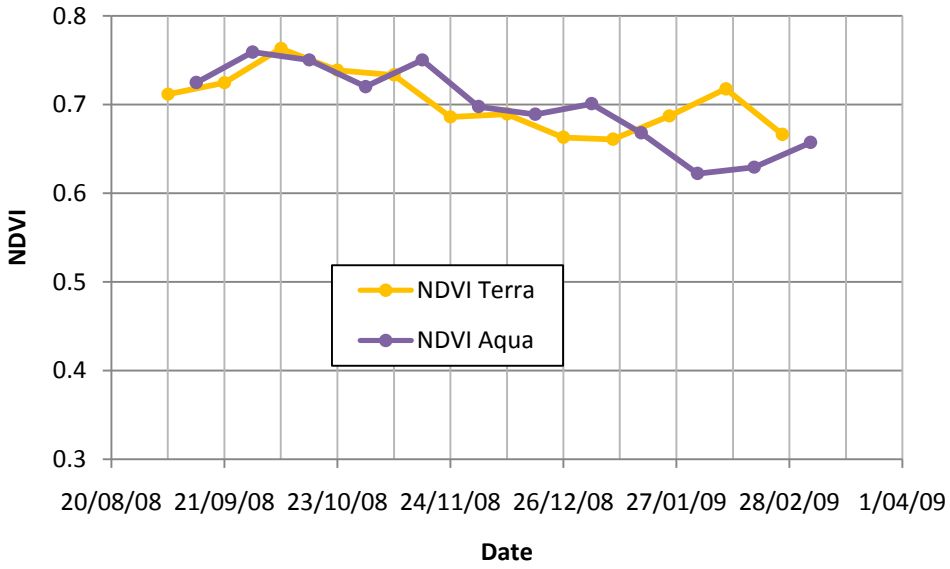

Figure 10: The seasonal course of NDVI from the Terra (morning) and Aqua (afternoon) data for 16 day periods for a well watered almond orchard. The almonds were harvested in March.

The almond trees' canopy development began in September and finished in December.**Error! Reference source not found.** Between the start and end of canopy growth there was little change in the values of NDVI. A dense matt of groundcover was present in the inter-row from the start of September until it was killed with weedicide in late November. Both measures of NDVI reach their peak values in early October.

During the development of the almond canopy between September and November the seasonal course of the NDVI derived from either the mid-morning or the mid-afternoon satellite overpass did not align with the seasonal courses of the ratio of ET:ETo determined for either the hour period (which encompassed the time of the satellite overpass) or for the 24 hour period, see Figure 11 and Figure 12 respectively. The values of the ET:ETo for the 24 hour period reached its peak value in late December. In December the value of the ET:ETo

determined for the 24 hour period encompassing the time of the satellite overpasses rose, whereas the value of NDVI fell.

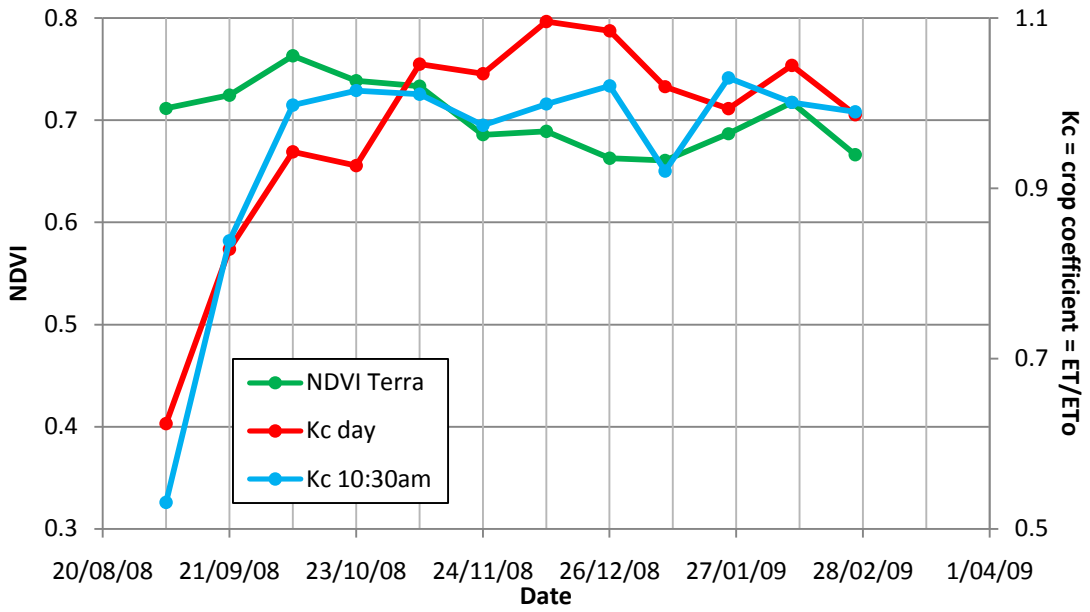

Figure 11: The seasonal course of NDVI from a mid-morning satellite overpass, the averages for the same sampling dates of the ratio ET:ETo for the hour period which encompasses the time of the satellite overpass and for the 24 hour period including the time of the satellite overpass.

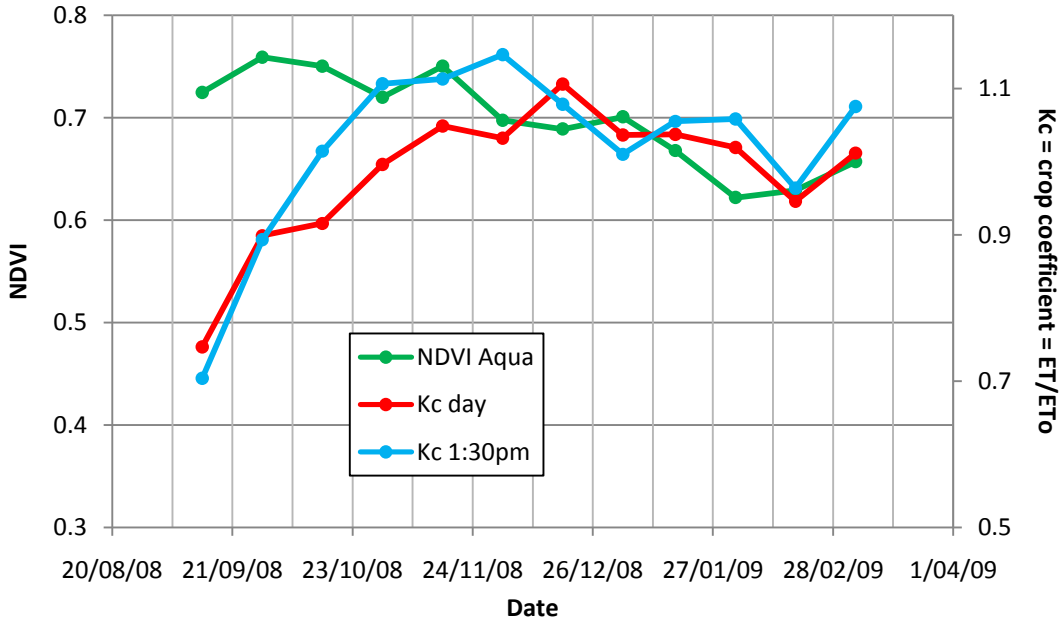

Figure 12: The seasonal course of NDVI from a early-afternoon satellite overpass, the averages for the same sampling dates of the ratio ET:ETo for the hour period which encompasses the time of the satellite overpass and for the 24 hour period including the time of the satellite overpass.

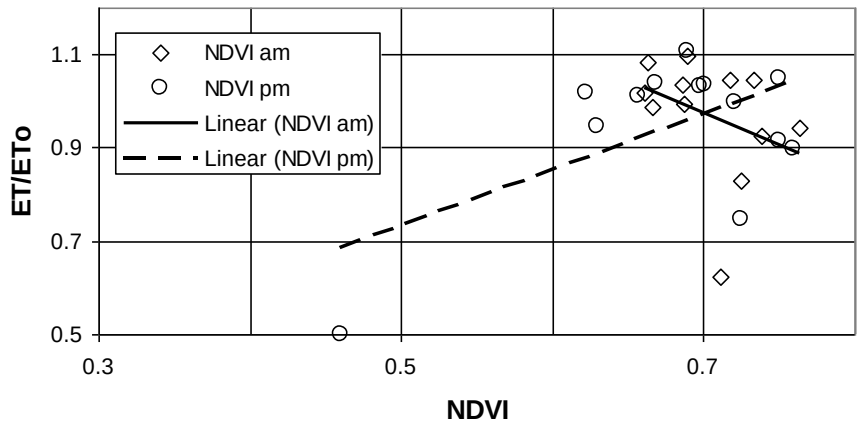

Figure 13: The relationship between 16 day averages of daily ET/ETo and NDVI's derived from Terra (morning) and Aqua (afternoon) satellite overpasses.

NDVI's from both mid-morning and mid-afternoon satellite overpasses were poor predictors of the values of ET:ETo, see Figure 13. The regressions between ET:ETo and mid-morning values of NDVI were not significant (P = 0.28) and whilst that between ET:ETo and mid-afternoon values of NDVI was just significant (P = 0.04) it only accounted for 28% of the variation in ET:ETo.

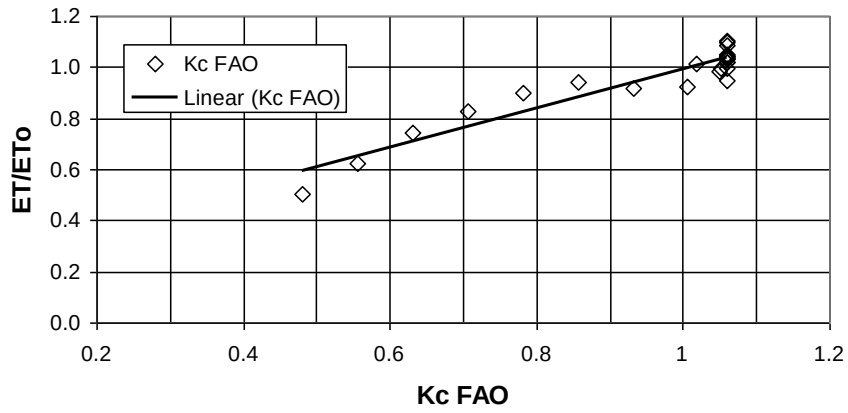

Figure 14: The relationships between 16 day averages of daily ET/ETo and FAO Kc's for the almond orchard.

Figure 14 shows the relationship between 16 day average daily ET/ETo and the FAO almond orchard Kc's. It is described by the regression equation

ET/ETo = 0.76*Kc+0.22 (r^2=0.89, n = 25, P<0.001),

The FAO Kc's were a better predictor of the ratio of ET/ETo than NDVI for almond orchards.

4. Conclusion

The seasonal course of values of NDVI determined from mid-morning overpasses of the Terra satellite is similar to that from early afternoon overpasses of the Aqua satellite for both the well watered vineyard and almond orchard. Therefore data acquired from either morning or afternoon satellite overpasses is suitable for use in investigating the relationship between ET/ETo and NDVI.

In the vineyard, the values of both ET/ETo and NDVI rose through the growing season. Values of NDVI derived from either the mid-morning or afternoon satellite overpasses were proportional to the ratios of ET:ETo determined for the hour periods during which the satellites made their overpasses.

The same cannot be said for the almond orchard. The seasonal course of the NDVI derived from the morning and afternoon satellite overpass did not align as well with the seasonal courses of the ratio of ET:ETo determined for either the hour period, which encompassed the time of the satellite, overpass or for the 24 hour period for the almond orchard compared to the vineyard.

More than one year of data is needed in order to make a comprehensive comparison between the Kc and NDVI. The data from both the almond orchard and the vineyard have shown correlations between the NDVI and Kc throughout the growing season, however those from the almond orchard were weak. In the vineyard NDVI values accounted for more of the variation in the 16 day average of daily ET/ETo than did the FAO Kc's for a wine grape vineyard. In contrast, for the almond orchard, the FAO Kc's accounted for much more of the variation in the ratio ET/ETo than did the NDVI.

It is likely that the water use of the studied vineyard can be estimated from measures of reference crop evapotranspiration and satellite derived NDVI.

5. References

ALLEN, G. A., PEREIRA, L. S., RAES, D. & SMITH, M. (1998) Crop evapotranspiration - Guidelines for computing crop water requirements. *FAO Irrigation and drainage paper 56.* Rome, FAO Food and Agricultural Organization of the United Nations.

AYARS, J. E., JOHNSON, R. S., PHENE, C. J., TROUT, T. J., CLARK, D. A. & MEAD, R. M. (2003) Water Use by Drip-irrigated Late-saeson Peaches. *Irrigation Science,* 22**,** 187-194.

BURBA, G., JASON, H. A. & PIDWIRNY, M. (2006) Evapotranspiration. *The Encyclopedia of Earth, http://www.eoearth.org/article/Evapotranspiration.*

GLEN, P. E., HUETE, R. H., NAGLER, P. L. & NELSON, S. G. (2008) Relationship between Remotely-sensed Vegetation Indices, Canopy Attributes and Plant Physiological Processess: What Vegetation Indices Can and Cannot Tell Us About the Landscape *Sensors,* 8**,** 2136-2160.

GOODWIN, I., WHITFIELD, D. M. & CONNER, D. J. (2006) Effeacts of Tree size on Water Use of Peach (*Prunus Persica* L. Batsch). *Irrigation Science,* 24**,** 59-68.

MARYLAND, U. O. (2008) Estimated Absorption Speatra. *Department of Physics.* http://www.physics.umd.edu/grt/taj/104a/greenleaves.png.

MDBMC (2007) Basin Tour. IN COUNCIL, M.-D. B. M. (Ed.), http://www2.mdbc.gov.au/about.1.html.

ODIS (2007) Healthy Vegetation Reflectance/ Stressed Vegetation Reflectance. On Demand Imagery Solutions, http://odis.ca/images/NDVI.jpg.

ORNL (2009) MODIS Global Subsets: Data Subsetting and Visualization. *MODIS Land Products Subsets.* The Oak Ridge National Laboratory Distributed Active Archive Center (ORNL DAAC)

ORNL (2010) MODIS Global Subsets: Data Subsetting and Visualization. *MODIS Land Products Subsets.* The Oak Ridge National Laboratory Distributed Active Archive Center (ORNL DAAC)

SSEC (2010) Space Science and Engineering Center. *http://www.ssec.wisc.edu/datacenter/.* University of Wisconsin-Madison.

TOWSON (2010) Remote Sensing Tutorial. *Remote Sensing Princples.* Center for GIS, Towson University, CGIS at Towson University.

TROUT, T. J. & JOHNSON, L. F. (2007) Estimating Crop Water use from Remotely Sensed NDVI, Crop Models, and Reference ET. *2007 USCID Fouth International Conference on Irrigation and Drainage.* Sacramento, California, U>S> Committee on Irrigation and Drainage.

TROUT, T. J., JOHNSON, L. F. & GARTUNG, J. (2008) Remote Senseing of Canopy Cover in Horticultural Crops. *Hortscience,* 43**,** 333-337.

WEIER, J. & HERRING, D. (2010) Measuring Vegetation (NDVI & EVI) *Earth Observatory.* NASA.

WILLIAMS, L. E. & AYARS, J. E. (2005) Grapevine Water Use and the Crop Coefficient are Linear Funtions of the Shaded Area Measured Beneath the Canopy. *Agricultural and Forest Meteorology,* 132**,** 201-211.

YALE (2007) Obtaining and Processing MODID Data. *Yale Institute of Biospheric Studies (YIBS) Research Centers.* Environmental Science Center, Center for Earth Observation, Yale University.

Appendix 1 - Evapotranspiation

Note, ETo shown in the following figures is derived from tower site values which are acquired above crop. These values vary slightly from the two meter AWS calculated reference crop values.

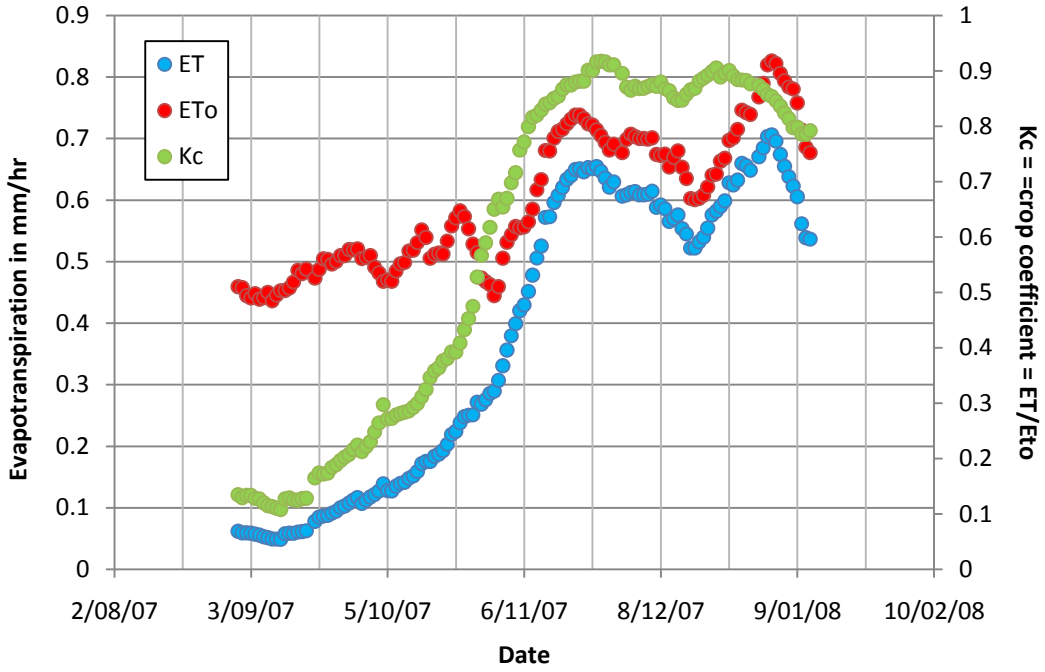

Figure 15: The relationship between ET (blue dots), ETo (red dots) and Kc (green dots) for the 16 day average hourly (morning) period for the well watered vineyard, Styles, Stevens & Grigson (unpublished data).

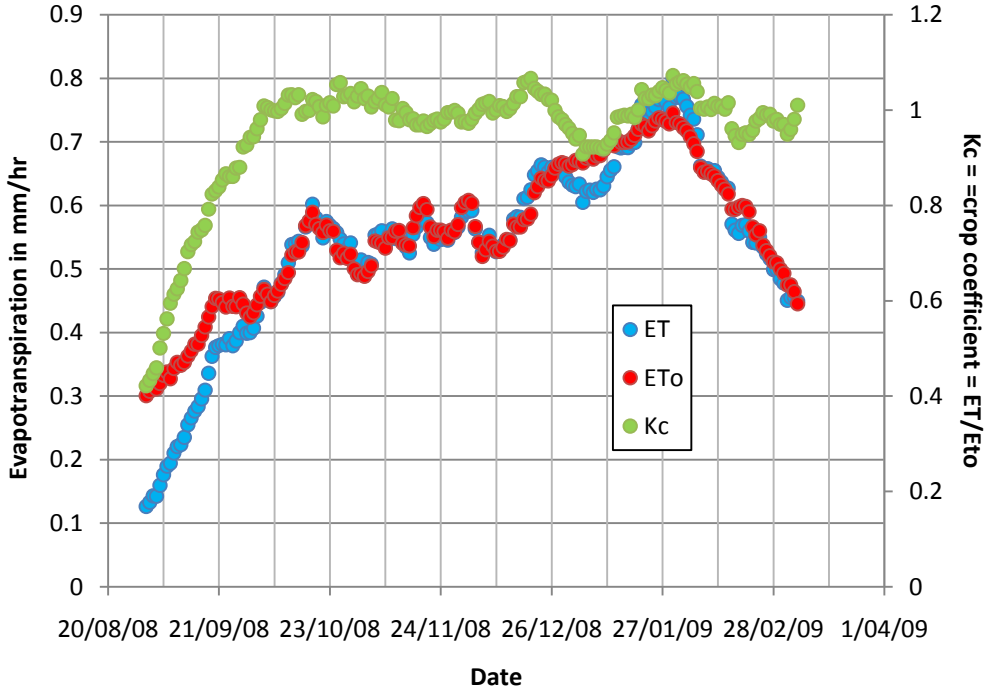

Figure 16: As in Figure 15 but for the hourly (morning) period for the well watered almond orchard, Ewenz, Stevens & Grigson (unpublished data).

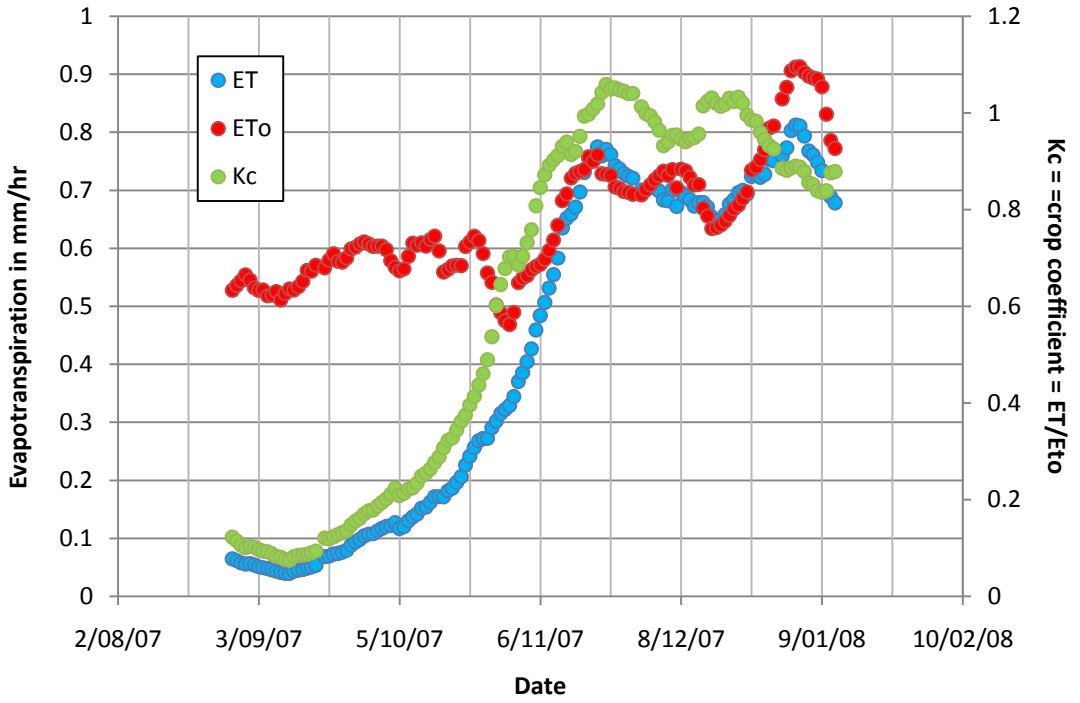

Figure 17: As in Figure 15 but for the hourly (afternoon) period for the well watered vineyard, Styles, Stevens & Grigson (unpublished data).

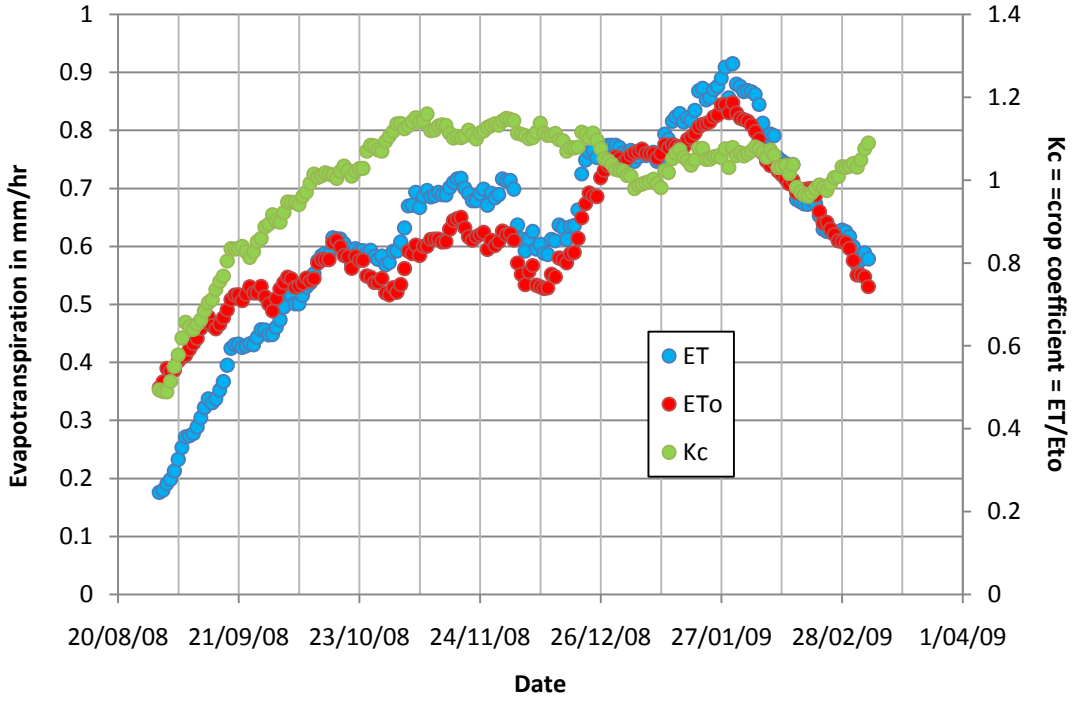

Figure 18: As in Figure 15 but for the hourly (afternoon) period for the well watered almond orchard, Ewenz, Stevens & Grigson (unpublished data).

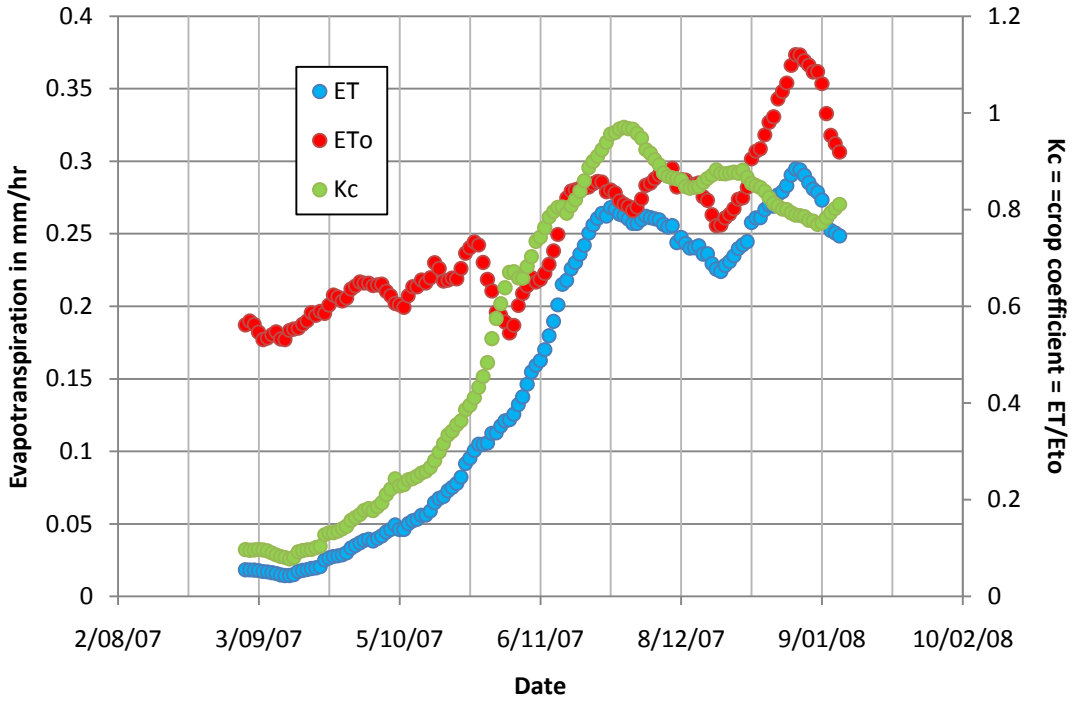

Figure 19: As in Figure 15 but for the 24 hour period for the well watered vineyard, Styles, Stevens & Grigson (unpublished data).

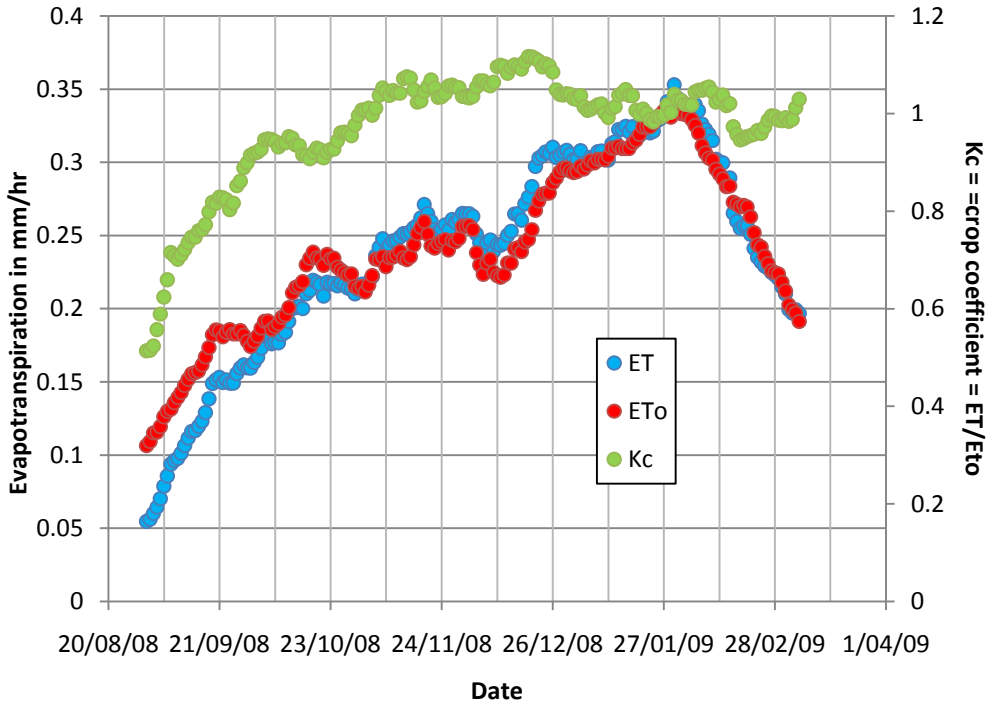

Figure 20: As in Figure 15 but for the 24 hour period for the well watered almond orchard, Ewenz, Stevens & Grigson (unpublished data).

Appendix 2 - Footprints

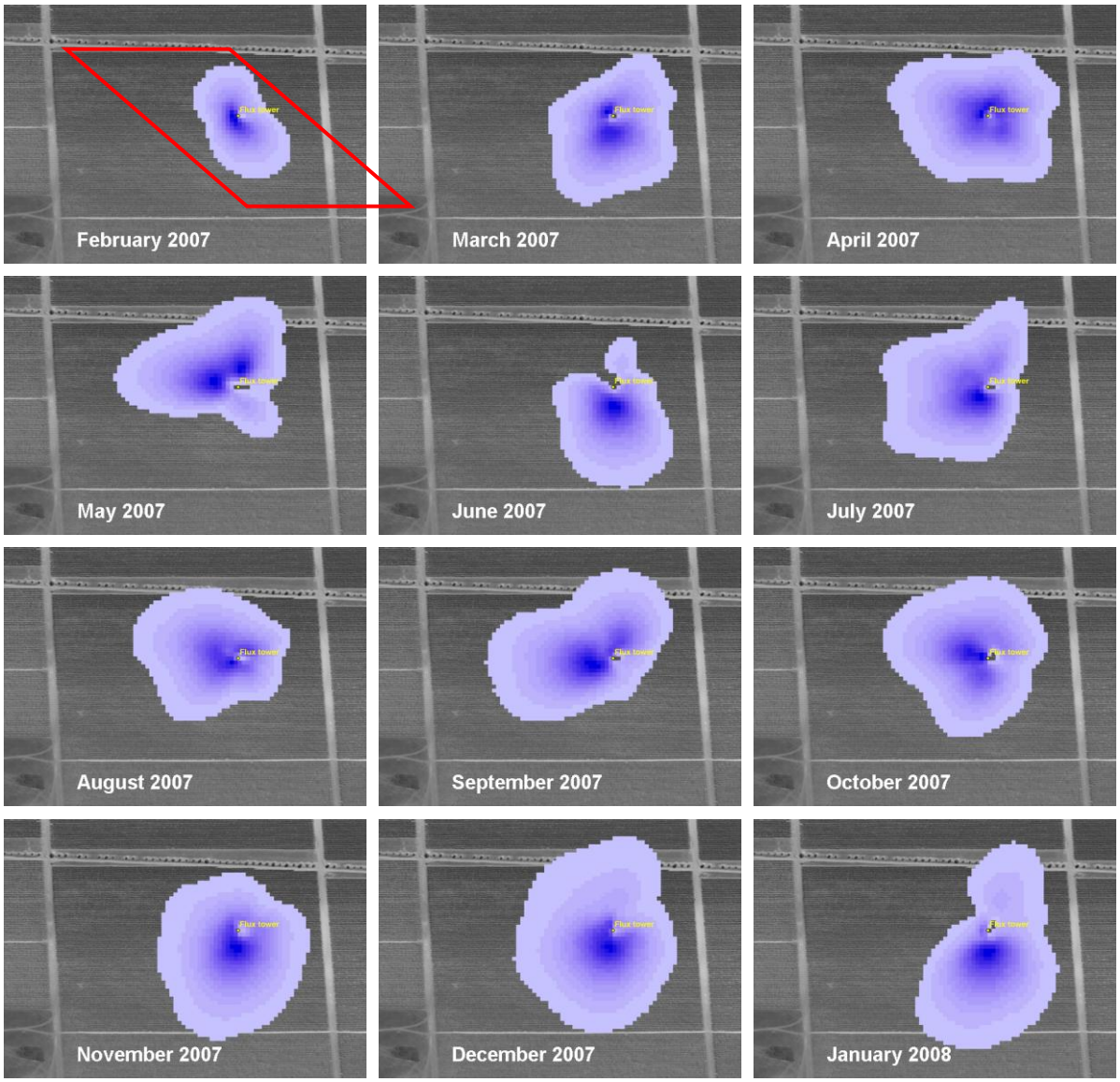

Figure 21: The ET-weighted composite measurement footprints showing approximately 85% of the area of influence for each month of measurements from February 2007 to January 2008 for the vineyard. Block length is approximately 400 m in the *x* direction and 280 m in the *y* direction. The red parallelogram overlaying the top left footprint exhibits the satellite tile, Styles, Stevens & Grigson (unpublished data).

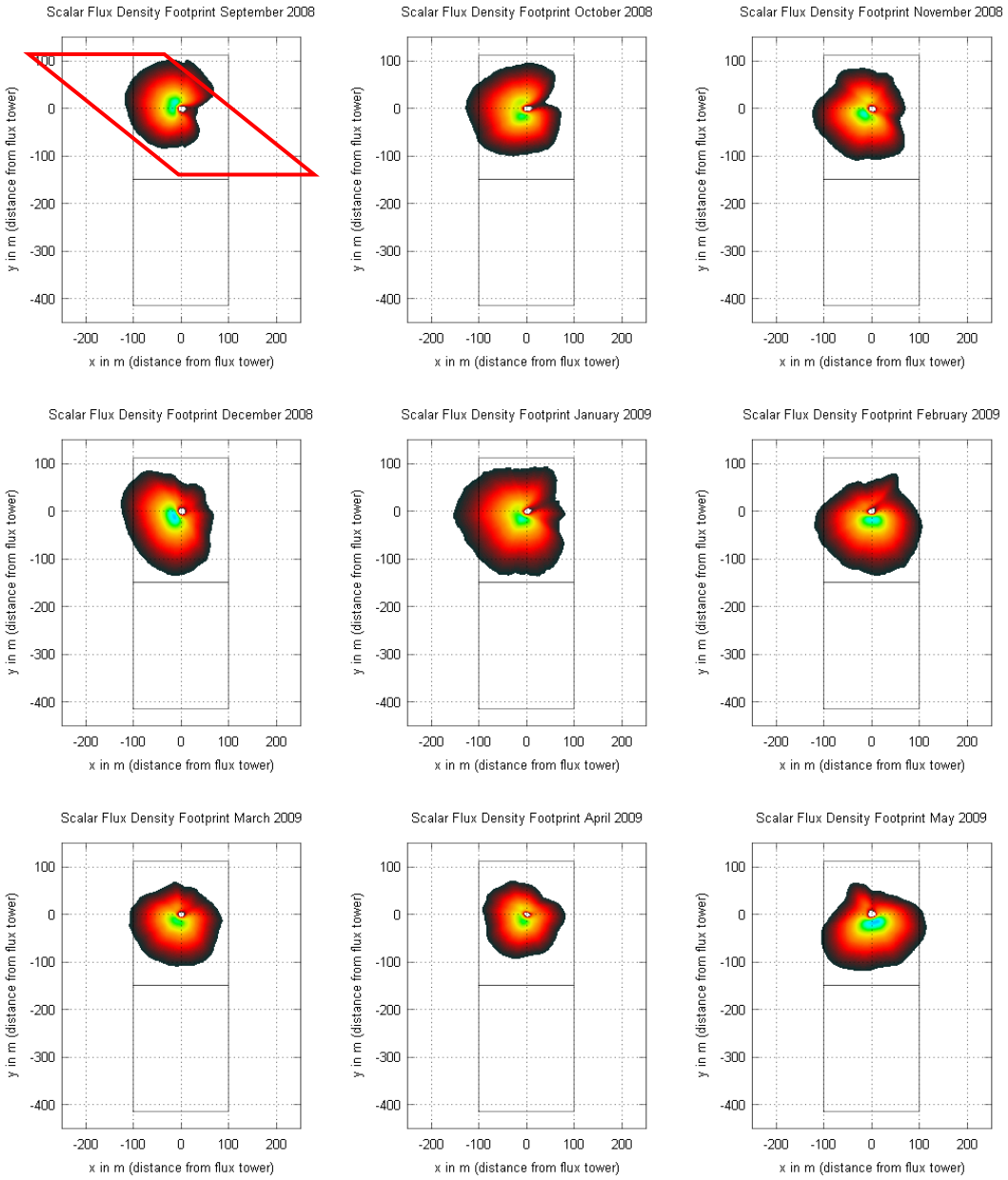

Figure 22: The ET-weighted composite measurement footprints showing approximately 95% of the area of influence for each month of measurements from September 2008 to May 2009 for the almond orchard. Indicated is the orchard section (northern rectangle, 200m by 250m) for the EC tower. The red parallelogram overlaying the top left footprint exhibits the satellite tile, Ewenz, Stevens & Grigson (unpublished data).

Appendix 3 - Soil Water Content

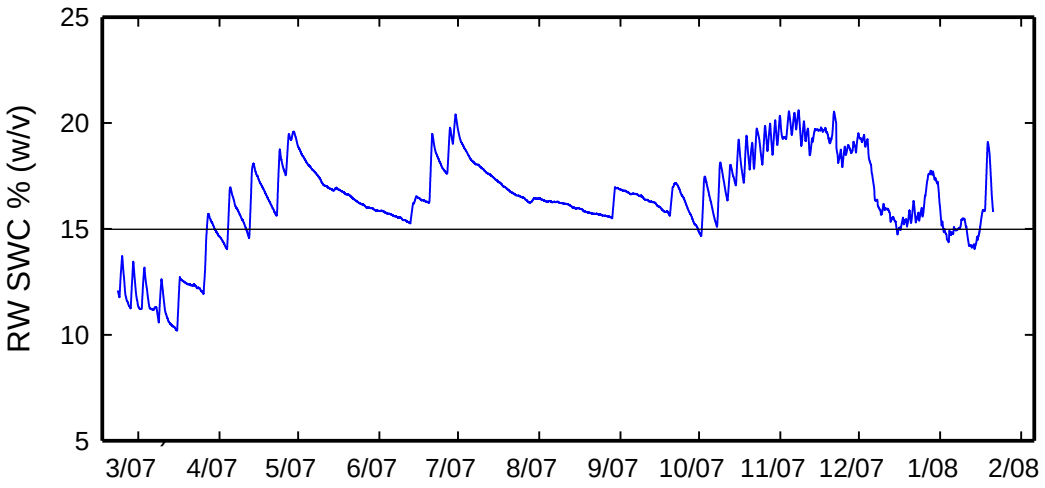

Figure 23: The root weighted soil water content 0 to 120cm depth in the vineyard, Styles, Stevens & Grigson (unpublished data).

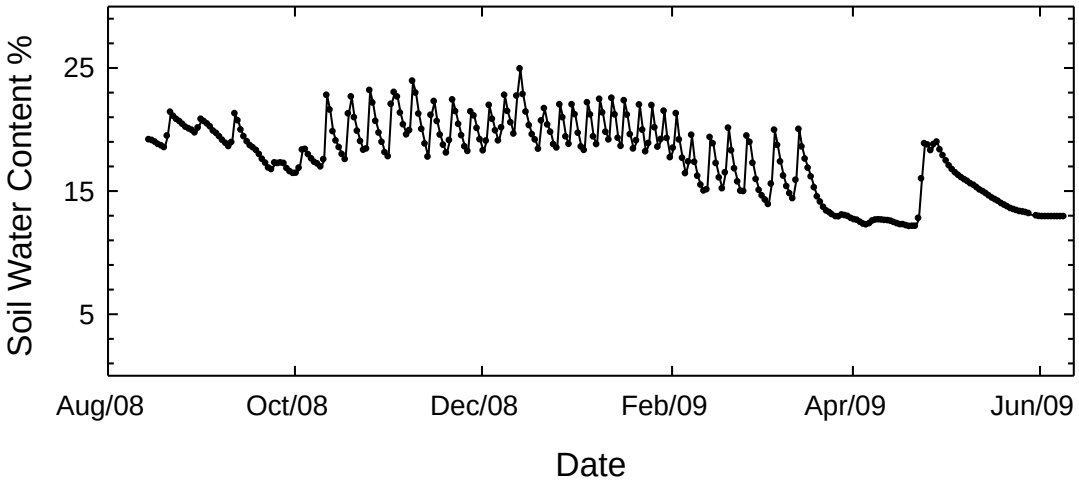

Figure 24: The soil water content average over 0 to 100cm depth in the almond orchard, Ewenz, Stevens & Grigson (unpublished data).

Appendix 4 - Pre-dawn Leaf Water Potential

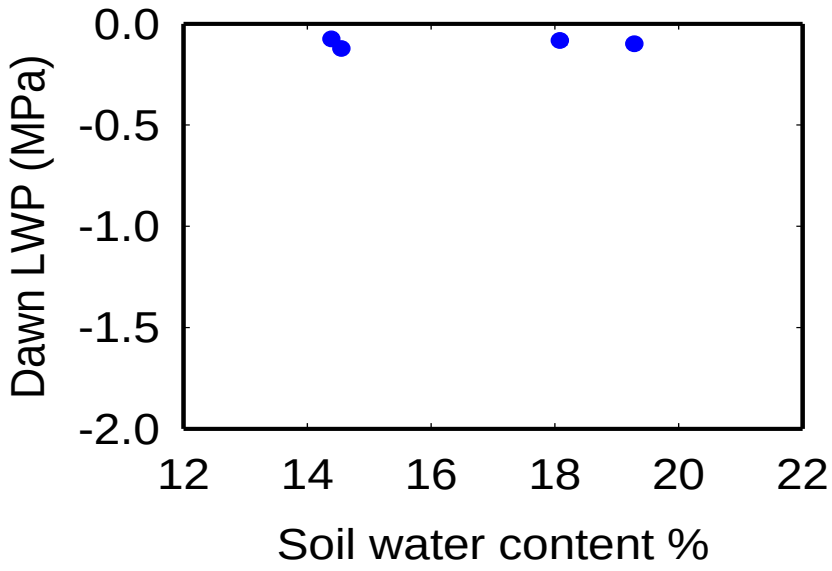

Figure 25: The variation in grapevine dawn leaf water potential with soil water content, Styles, Stevens & Grigson (unpublished data).

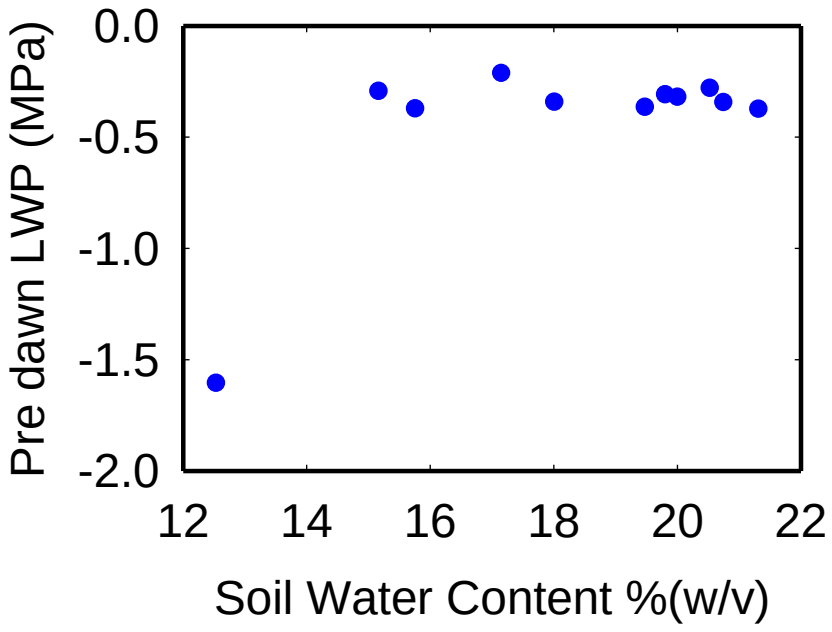

Figure 26: The variation in almond pre-dawn leaf water potential with soil water content, Ewenz, Stevens & Grigson (unpublished data).

Appendix 5 - Satellite Overpasses

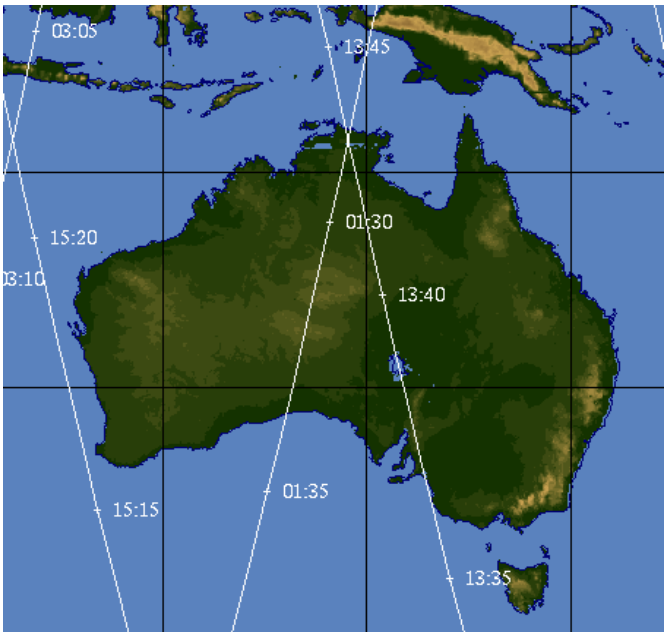

Figure 27: Terra's predicted pathway; passes on 1/5/2008. The time is in universal time coordinated (UTC) (SSEC, 2010).

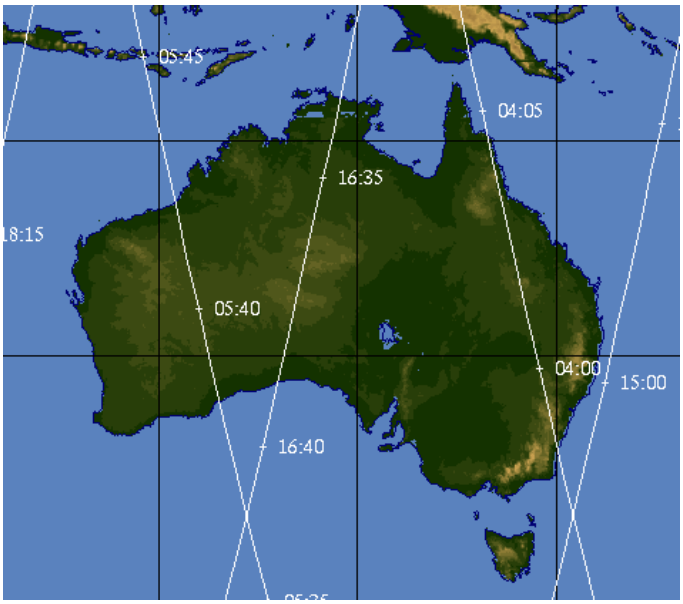

Figure 28: Aqua's predicted pathway; passes 1/4/2008. The time is in universal time coordinated (UTC) (SSEC, 2010).

Appendix 6 - Collecting MODIS data

MODIS data was collected through the Oak Ridge National Laboratory Distributed Active Archive Centre (ORNL DAAC) website (ORNL, 2009).

This site is sponsored by NASA for use in areas such as environmental research. On the home page there is a link under 'Get Products,' click on 'Get MODIS Land Product Data.' Then under 'Get Subsets' click on 'Create Subset.' The following image should appear on the screen.

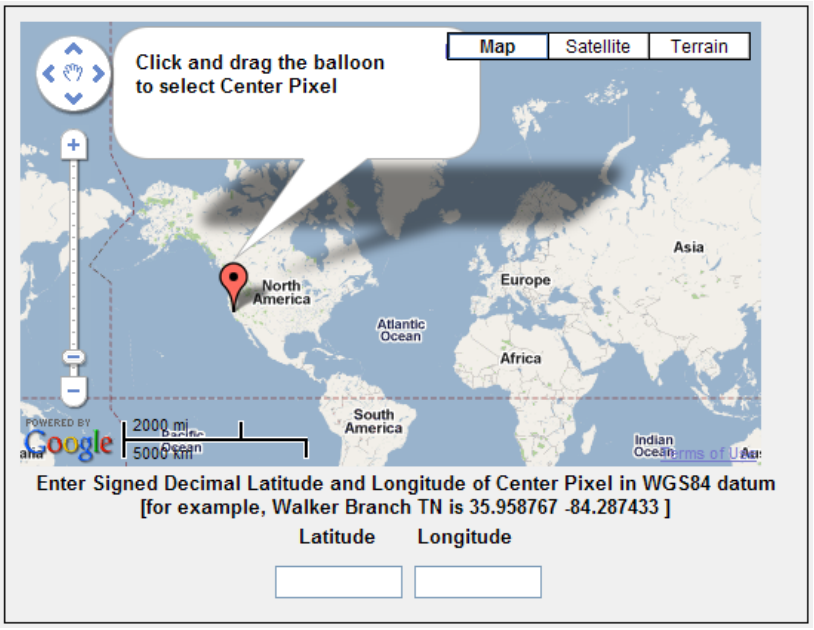

Figure 29: Map of the earth (ORNL, 2009)

The balloon can then be dragged to the place of interest, i.e. Loxton, and by using the satellite option the exact location of the vineyard or almond orchard and the eddy covariance tower can be found.

The tiles for NDVI for both the vineyard and almond orchard were aligned with the footprint for the instruments used in the measurement of crop ET (see Appendix 1).

Once the area of interest has been located, press continue. Both [MOD13Q1] Vegetation Indices (NDVI, EVI) and [MYD13Q1] Vegetation Indices (NDVI, EVI) were chosen in turn as the first represents the morning (Terra) data and the second represents the afternoon (Aqua) data. To specify the number of kilometres encompassing the centre location 0, 0 was chosen so that only one tile would be displayed, that is 250m by 250m.

After continuing to the next page, the dates of interest and the ”Generate GeoTIFF in MODIS Sinusoidal Projection” were chosen. The data can then be sent to an email address ready to be sorted.

Raw data obtained through the ORNL DAAC website (ORNL, 2010) was sorted into an excel spread sheet to give the blue band, red band, near-infrared band, the NDVI and the EVI for the years between 2002 and 2009. This was done for both the morning (Terra) and afternoon (Aqua) data. As this site already calculates the NDVI and EVI there was no need to calculate them separately.